J Nanopart Res (2013) 15:1401
DOI 10.1007/s11051-012-1401-8

RESEARCH PAPER

Sonochemical fabrication of $CdSe_xTe_{1-x}$/Au nanotubes and their potential application in biosensing

Feng Lu · Shanhu Liu · Li-Ping Jiang · Jun-Jie Zhu

Received: 28 October 2012 / Accepted: 22 December 2012 / Published online: 5 January 2013

Abstract $CdSe_xTe_{1-x}$ semiconductor alloy nanotubes (with an external diameter of 140 nm and an internal diameter of 100 nm) were successfully prepared based on the sacrificial template of Cd(OH)Cl nanorods, and were further in situ assembled with gold nanoparticles (AuNPs) via a sonochemical approach to form the $CdSe_xTe_{1-x}$/Au nanotubes. The prepared $CdSe_xTe_{1-x}$/Au nanotubes were characterized by X-ray diffraction, field emission scanning electron microscopy, transmission electron microscopy, energy-dispersive spectrometry, and X-ray photoelectron spectra. $CdSe_xTe_{1-x}$/Au nanotubes could integrate the advantages of the electronic properties of CdSeTe and the biocompatible properties of AuNPs. A novel biosensor was fabricated after the immobilization of hemoglobin (Hb) on $CdSe_xTe_{1-x}$/Au nanotubes. The immobilized Hb exhibited fast direct electron transfer and good electrocatalytic performance to H_2O_2.

F. Lu · S. Liu · L.-P. Jiang · J.-J. Zhu (✉)
State Key Laboratory of Analytical Chemistry for Life Science, School of Chemistry and Chemical Engineering, Nanjing University, Nanjing 210093, People's Republic of China
e-mail: jjzhu@nju.edu.cn

S. Liu
e-mail: liushanhu@163.com

S. Liu
Institute of Environmental and Analytical Sciences, College of Chemistry and Chemical Engineering, Henan University, Kaifeng 475004, People's Republic of China

Keywords Sonochemical reduction · Alloyed nanotube · Gold nanoparticles · Biosensor

Introduction

In recent years, tubular inorganic nanostructures have attracted increasing attention due to their unique morphology for the fabrication of nanodevices and nanocarriers (Xia et al. 2003; Miao et al. 2007; Zhou et al. 2009). Among them, cadmium chalcogenide nanotubes can integrate the advantages of the tubular morphology and the unique physical properties of semiconductors, and then be pursued for their potentials as building blocks in the fields of solar cells, photoelectronic devices, catalysis, and biosensors (Rao et al. 2001; Mercuri et al. 2010; Shim et al. 2009). Several methods have been employed for the preparation of cadmium chalcogenide nanotubes, including template, sonoelectrochemical, and vapor deposition methods (Ding et al. 2009; Zhai et al. 2009; Miao et al. 2005; Shen et al. 2008; Huang et al. 2009). For instance, Zhou et al. synthesized vertically aligned CdSe nanotubes on indium tin oxide (ITO) glass using a ZnO nanorod array as the template (Zhou et al. 2009). Tang et al. reported the synthesis of CdTe nanotubes by hierarchical assembly of nanoparticles at the water–oil interface (Ding et al. 2009). Yu et al. developed a photochemical approach to generate CdS nanotubes (Huang et al. 2009). In our previous work,

we have obtained CdS and CdSe nanotubes via sonochemical methods (Miao et al. 2005; Shen et al. 2008). However, only a few reports have been found focusing on the synthesis of cadmium chalcogenide alloy nanotubes with controllable composition although the adjustment on the composition of semiconductors might bring some amazing electrical and optical properties (Liang et al. 2009a; Farvid et al. 2011).

On the other hand, native redox protein does not easily undergo facile redox reactions at bare electrode because the electroactive prosthetic groups are deeply buried within the protein structure, producing an unfavorable orientation and leading to the absorption of impurities on the electrode surface (Zhang et al. 2007a, 2007b; Xiao et al. 2009; Yang et al. 2008; Zhao et al. 2010). Gold nanoparticles (AuNPs) have been proved to offer a robust microenvironment for the immobilization of protein in virtue of their biocompatibility and unique electronic properties (Jha and Ramaprabhu 2010; Cai et al. 2006; Cui et al. 2008a). After AuNPs were further incorporated on an appropriate host matrix, fast direct electron transfer between the protein and the electrodes could be observed (Zhang et al. 2011). Currently, various synthetic routes have been developed to incorporate AuNPs on the host matrix through noncovalent/covalent modifications, layer-by-layer deposition, electrochemical deposition, or using homogeneous silica shell as linker (Jia et al. 2008; Chang et al. 2009; Lo et al. 2010; Ren et al. 2010; Yang et al. 2010; Zhu et al. 2009). However, these synthetic routes are often complicated and lead to the presence of the insulation layers (such as silane coupling agent, polymer and surfactant) between the host matrix and AuNPs, which tends to block the electron transport pathway. Therefore, it is highly desirable to develop a facile and efficient route for the in situ incorporation of AuNPs on the host matrix. Ultrasound as a powerful tool to prepare nanomaterials has been widely used for the in situ synthesis of gold nanoparticles on iron oxide and silica (Pradhan et al. 2008; Mizukoshi et al. 2008; Chen et al. 2001). However, to the best of our knowledge, there is no report on using sonochemical method for the in situ decoration of gold nanoparticles on cadmium chalcogenide nanotubes.

In this work, $CdSe_xTe_{1-x}$/Au nanotubes were prepared and $CdSe_xTe_{1-x}$/Au/Hb biocomposites were fabricated according to the procedure shown in scheme 1. The Cd(OH)Cl nanorods were fabricated by a facile precipitation route (Miao et al. 2007, 2005), and used as the sacrificial templates for the fabrication of $CdSe_xTe_{1-x}$ nanotubes. The component in the alloy nanotubes could be tuned by adjusting the initial ratio of Se and Te. Then AuNPs were in situ decorated on the alloy nanotubes via a sonochemical approach without a bridge insulation layer. After that, The $CdSe_xTe_{1-x}$/Au nanotubes were further used for loading Hb to fabricate a biosensor. The immobilized Hb exhibited fast direct electron transfer and good electrocatalytic performance to H_2O_2 with high sensitivity and wide linear range.

Experimental section

Materials

Selenium powder (Se, 99.5 %, 200 mesh) and tellurium powder (Te, 99.8 %, 200 mesh) were purchased from Acros Organics (USA). $CdCl_2$, NaOH, $NaBH_4$, and Hb were purchased from Sigma-Aldrich Chemical Reagent Co., Ltd. $HAuCl_4$ and Poly (vinylpyrrolidone) (PVP) was from Shanghai Chemical Reagent Co. (Shanghai, China). All other chemicals were of analytical grade and used without further purification. Millipore water (18.2 MΩ cm at 25 °C) was used throughout all experiments.

Preparation of $CdSe_xTe_{1-x}$/Au nanotubes

For the synthesis of Cd(OH)Cl nanorods, $CdCl_2$ (0.25 mol) was added into the PVP aqueous solution (3 %, 30 mL). Then, NaOH solution was added dropwise into the above solution under stirring. The obtained white precipitate was aged at 90 °C overnight, washed with distilled water and ethanol, and

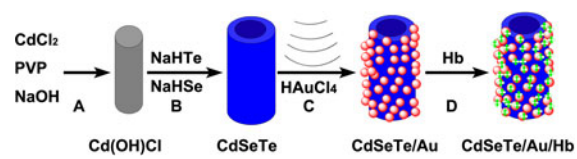

Scheme 1 Schematic illustration of the fabrication process of the $CdSe_xTe_{1-x}$/Au/Hb biocomposites. *a* Synthesis of Cd(OH)Cl nanorods. *b* Preparation of $CdSe_xTe_{1-x}$ nanotubes. *c In situ* decoration of AuNPs via a sonochemical method. *d* Assembly of Hb on the $CdSe_xTe_{1-x}$/Au nanocomposite

dried under vacuum at room temperature before characterization and application (Step A).

For the synthesis of $CdSe_xTe_{1-x}$ nanotubes, the as-prepared Cd(OH)Cl nanorods (0.25 g) were added into 30 mL of freshly prepared NaHTe/NaHSe (0.03 M respectively) solution in a round-bottomed flask. The reaction was carried out in nitrogen protection at 60 °C for 1 h. After that, the precipitates were centrifuged and washed sequentially with distilled water and acetone (Step B). The composition of $CdSe_xTe_{1-x}$ nanotubes could be adjusted by controlling the initial ratio of NaHTe and NaHSe.

For the preparation of $CdSe_xTe_{1-x}$/Au nanotubes, 50 mg of the as-prepared nanotubes were dispersed into 10 mL of water, followed by adding 1.5 mL of chloroauric acid (1 % $HAuCl_4$ solution). The mixture was put in an ultrasonic cleaner (KQ218, Kun Shan Ultrasonic Instruments Co., Ltd.) for 30 min and kept static at room temperature for 1 h until the Au precursor was reduced completely (Step C). Then, the solution was centrifuged and washed several times and dispersed in water (5 mg mL^{-1}).

Preparation of $CdSe_xTe_{1-x}$/Au/Hb biocomposites

5 mg of $CdSe_xTe_{1-x}$/Au nanotubes was added to the Hb solution (5 mg mL^{-1} in 10 mM PBS, pH 7) and shaken for 1 h for protein absorption. The biocomposites were then centrifuged and washed with PBS for three times (Step D).

Fabrication of the biosensor

The glass carbon electrode (GCE) was first polished with 1.0, 0.3, and 0.05 μm alumina slurry successively and rinsed with water completely. 10 μL of the $CdSe_xTe_{1-x}$/Au/Hb suspension (10 mg mL^{-1}) was deposited on the pretreated GCE surface and dried in a silica gel desiccator. 5 μL of Nafion solution (0.5 %) was added for immobilization of the biocomposites. Finally, the electrode was left to dry at 4 °C overnight.

Instrumentation

Field emission scanning electron microscopy (FE-SEM) images were obtained using Hitachi S-4800 at an accelerating voltage of 10 kV. Transmission electron microscopy (TEM) images and selected area electron diffraction (SAED) patterns were taken using a JEOL JEM-2100 at an accelerating voltage of 200 kV. X-ray powder diffraction (XRD) measurements were performed on a Japan Shimadzu XRD-6000 with Cu Kα radiation ($\lambda = 0.15418$ nm); a scanning rate of 0.05° s^{-1} was applied to record the patterns in the 2θ range of 20–70°. X-ray photoelectron spectra (XPS) were obtained using a Thermo ESCALAB 250 electron spectrometer with 150 W monochromatized Al Kα radiation (1486.6 eV). The binding energy of C1 s level from contamination of saturated hydrocarbons at 284.8 eV was used as internal reference to calibrate the spectra. Electrochemical experiments were performed using a CHI660a workstation (Shanghai Chenhua, China) using a conventional three-electrode system, using a platinum wire as the auxiliary, a saturated calomel electrode as the reference, and the modified GCE as the working electrode. Electrolyte solutions were deoxygenated before and during measurements.

Results and discussion

Characterization of the as-prepared $CdSe_xTe_{1-x}$ nanotubes

The morphology and phase analysis of Cd(OH)Cl nanorods were investigated by FESEM and XRD. It can be observed from Fig. 1a that the products show a rod-like structure with diameter of about 110 nm. The XRD patterns is shown in Fig. 1b and all the diffraction peaks can be indexed to the hexagonal phase of Cd(OH)Cl (JCPDS: 74-1047).

The prepared Cd(OH)Cl nanorods were used as the sacrificial templates for the $CdSe_xTe_{1-x}$ nanotubes, and were gradually consumed, meanwhile the resultant chalcogenide formed a shell structure around the templates, inheriting the outer shapes of the sacrificial templates. When the sacrificial templates were completely consumed, the chalcogenide nanotubes could be obtained. The structure and composition of the nanotubes were investigated by SEM and TEM images. A typical SEM image in Fig. 2a reveals that the $CdSe_xTe_{1-x}$ nanotube has an external diameter of about 140 nm and an internal diameter of about 100 nm, which is consistent with the diameter of the Cd(OH)Cl nanorods. The distinct contrast derived from the difference of electron density in TEM image (Fig. 2b) also confirms their tubular structures. The

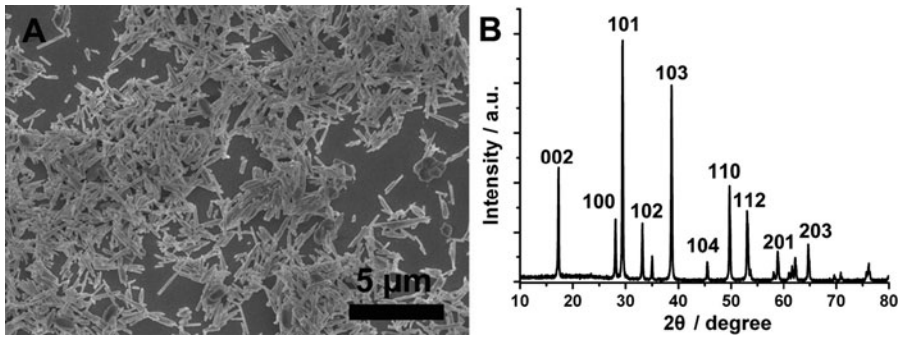

Fig. 1 SEM image (**a**) and XRD patterns(**b**) of Cd(OH)Cl nanorods

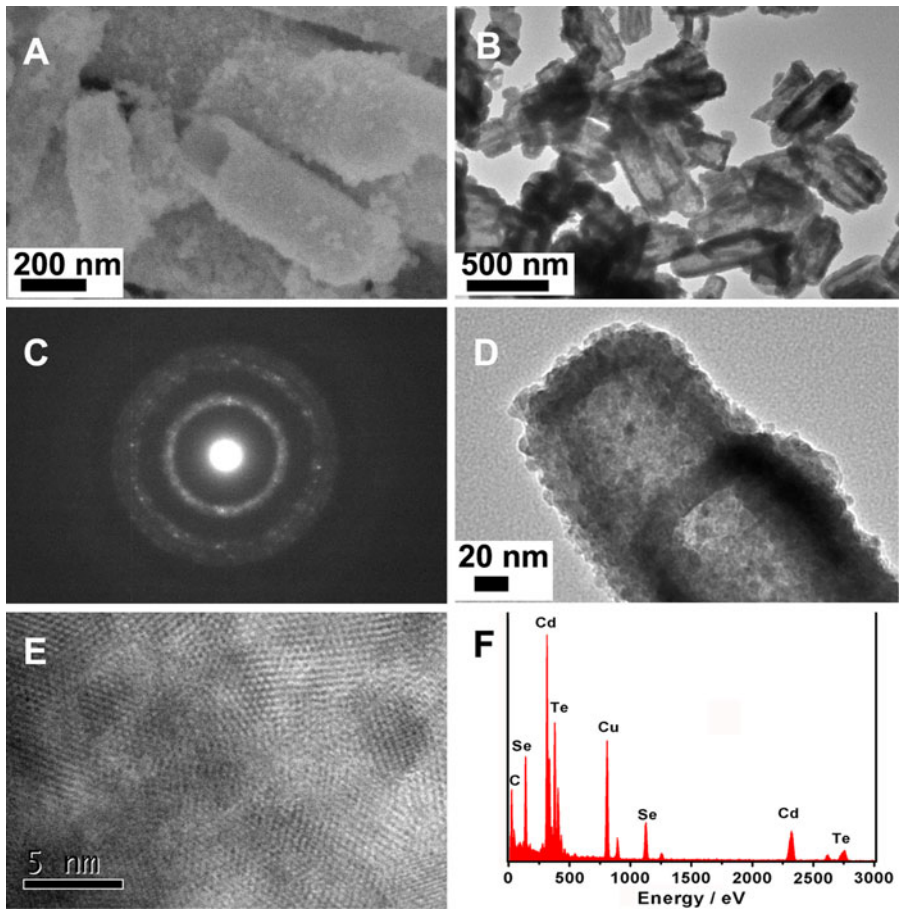

Fig. 2 SEM image (**a**), TEM image (**b**), SAED patterns (**c**), HRTEM images (**d, e**) and EDS spectra (**f**) of $CdSe_xTe_{1-x}$ nanotubes

corresponding SAED patterns (Fig. 2c) show a set of diffraction rings which corresponds to the cubic phase of $CdSe_xTe_{1-x}$ with polycrystalline nature. The HRTEM investigation could provide further information about the microstructure of the nanotubes (Fig. 2d). The wall of the nanotubes is composed of numerous highly compacted nanoparticles with sizes of 4–6 nm, and the thickness of the wall is about 20 nm. A higher resolution image (Fig. 2e) shows that the nanoparticles with tube wall are well crystallized. As is shown in Fig. 2f, cadmium and selenium and tellurium elements were detected (carbon comes from

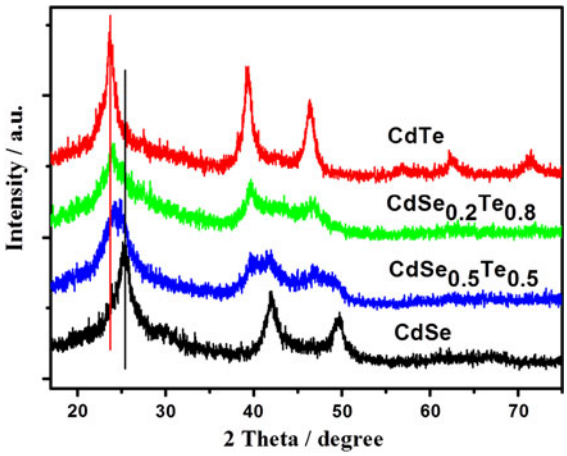

Fig. 3 XRD patterns of CdTe, CdSe, and $CdSe_xTe_{1-x}$ nanotubes with different ratios of selenium and tellurium. The *percentages* indicate the initial concentrations of Se and Te. The *vertical lines* represent XRD patterns of bulk CdTe (*bottom*, JCPDS 75-2086) and CdSe (*top*, JCPDS 19-0191)

the electric conductive adhesive used to immobilize the sample powder), and their atom ratio is about 1:0.57:0.45, which is similar to the initial ratio of NaHTe and NaHSe.

Figure 3 shows XRD patterns of the $CdSe_xTe_{1-x}$ nanotube with different ratios of Se and Te elemental. The XRD peaks for pure CdTe and CdSe are narrower and better defined than those for $CdSe_xTe_{1-x}$ nanotubes synthesized under identical conditions, which is consistent with an impurity-induced nanocrystals lattice disorder and a decrease in the average size of nanoparticles, suggesting that the presence of foreign ions inhibits nanocrystal growth even for ions that have similar chemical behavior (Farvid et al. 2011). The diffraction peaks gradually shifted to larger angles with the increase of Se molar fraction, which also indicated that the component can be adjusted by controlling the experiment conditions.

Characterization of the $CdSe_xTe_{1-x}$/Au nanocomposites

Sonochemistry has been extensively used in the synthesis of various nanomaterials (Shen et al. 2008; Qiu et al. 2004). In this work, this robust method was used for the in situ assembly of AuNPs. As shown in Fig. 4a, the numerous individual black nanodots spread along the nanotubes are AuNPs, indicating that AuNPs are successfully assembled on the surface of the $CdSe_xTe_{1-x}$ nanotubes. The corresponding SAED patterns (Fig. 4b) exhibit additional diffraction dots besides diffraction rings, which can be assigned to the (220) and (111) planes of gold nanocrystals. More evidence on the assembly of AuNPs was obtained from the HRTEM observation (Fig. 4c). The arrows marked are some gold nanoparticles with a diameter about 6 nm and d spacing of 0.24 nm, which was in good agreement with that for (111) planes of gold nanocrystals. The EDS analysis (Fig. 4d) was performed to confirm the composition of Au-$CdSe_xTe_{1-x}$

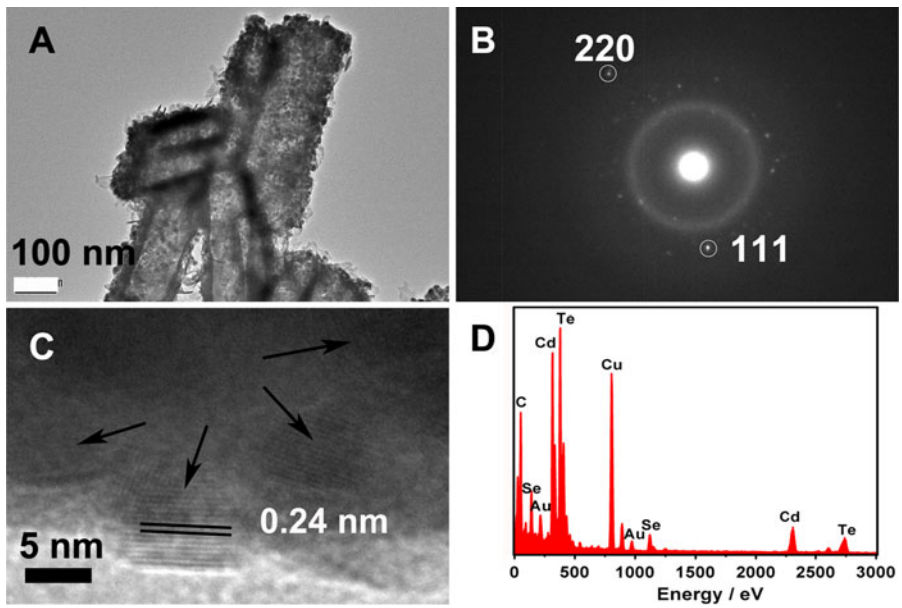

Fig. 4 TEM image (**a**), SAED patterns (**b**), HRTEM image (**c**), and EDX spectra (**d**) of $CdSe_xTe_{1-x}$/Au nanotubes

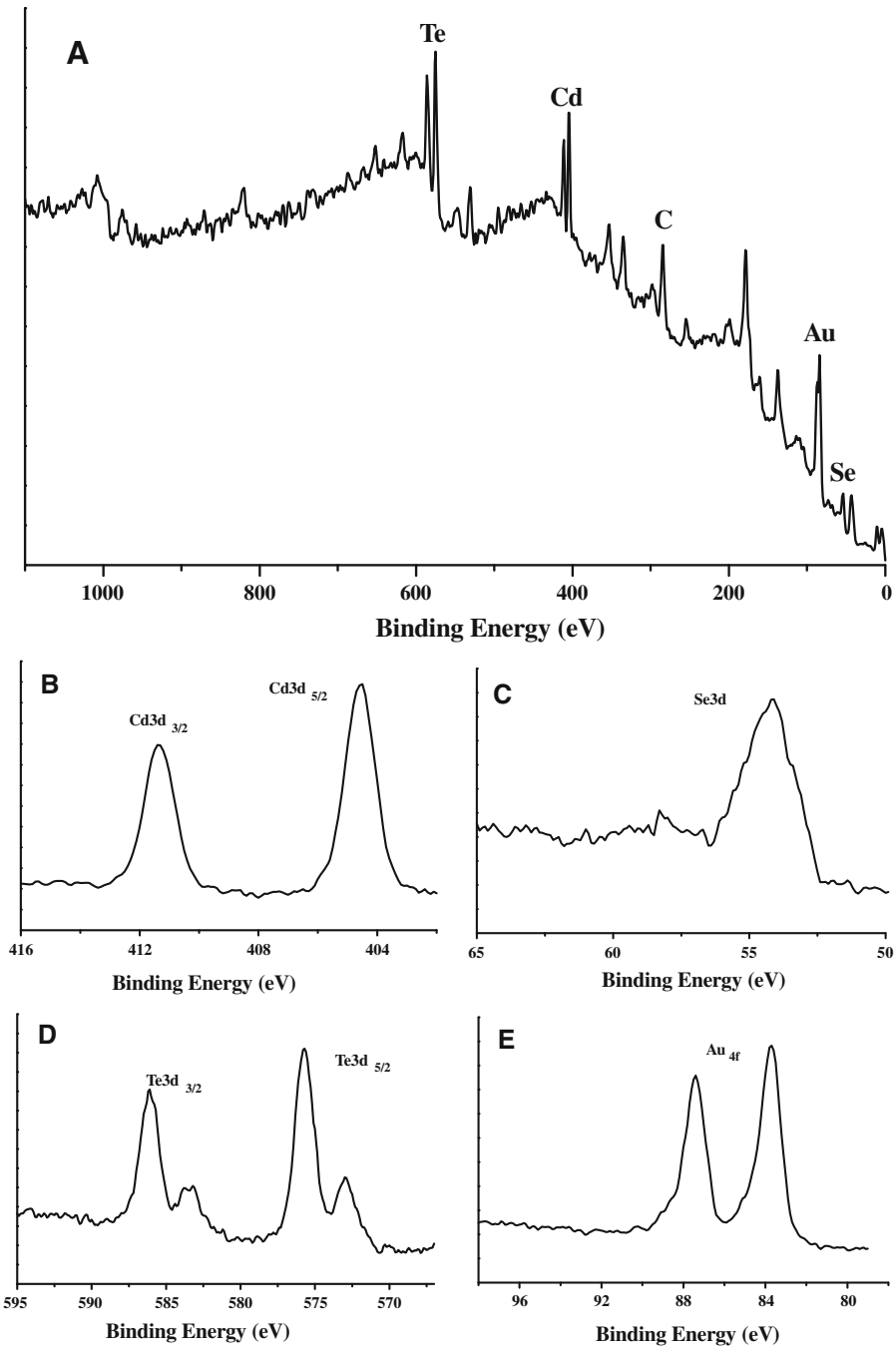

Fig. 5 XPS spectra of $CdSe_xTe_{1-x}$/Au nanotubes. **a** Survey; **b** Cd; **c** Se; **d** Te; **e** Au

nanotubes and each element (Cd, Se, Te, and Au) in the nanotubes was well identified.

The composition of the $CdSe_xTe_{1-x}$/Au nanotubes can be further identified by XPS spectroscopy, which is considered as a powerful tool for the identification of the chemical nature of the surface of nanomaterials (Liu et al. 2009, 2011). As shown in Fig. 5, two peaks centered at 411.8 and 405.1 eV correspond to Cd $3d_{3/2}$ and Cd $3d_{5/2}$ (Fig. 5a). The peaks at 54.3 eV is attributed to the Se_{3d} (Fig. 5b). The peaks around 586.10 and 575.70 eV are corresponding to Te $3d_{3/2}$ and Te $3d_{5/2}$, and the peaks at 83.6, 87.4 eV correspond to Au_{4f}. The XPS results are in good agreement with the reported values in the literature (Wang and Han 2010; Wang et al.

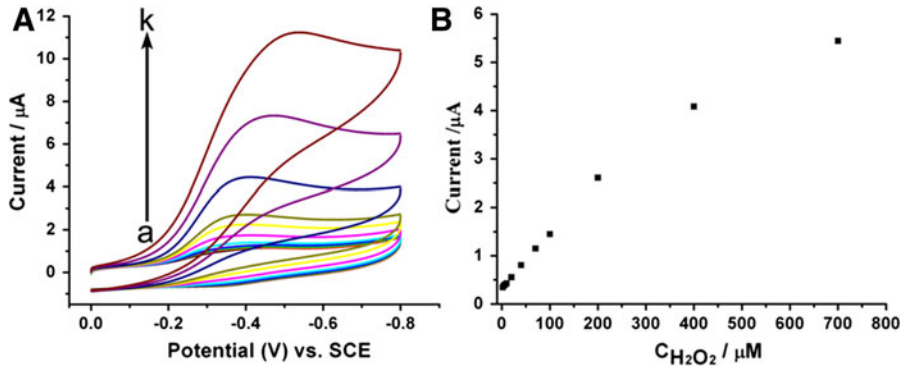

Fig. 6 Cyclic voltammograms (**a**) and the calibration curve (**b**) of $CdSe_xTe_{1-x}$/Au/Hb modified GCEs in 0.1 M PBS at pH = 7.0 in the presence of: (a) 2, (b) 4, (c) 7, (d) 10, (e) 20, (f) 40, (g) 70, (h) 100, (i) 200, (j) 400, and (k) 700 mM H_2O_2 at a scan rate of 200 mV s^{-1}

2009; Zeng et al. 2009; Cui et al. 2008b). It is reported that metal ions ($PtCl_6^{2-}$ or Pd^{2+}) can be reduced by Te nanowires forming Pt nanotubes or Pd nanowires, while Te was oxidized into TeO_3^{2-} (Liang et al. 2009b). Similarly, the formation of AuNPs on the surface of $CdSe_xTe_{1-x}$ nanotubes might be due to the weak reducibility of Se^{2-} and Te^{2-} ions in the nanotubes under ultrasonic condition. These nanocomposites with the multifunctional properties provided by $CdSe_xTe_{1-x}$ and decorated AuNPs, may have many applications such as biosensors, electrocatalysis, and so on.

Assembly of Hb onto the $CdSe_xTe_{1-x}$/Au nanotubes for biosensing

$CdSe_xTe_{1-x}$/Au nanotubes inherited the advantages from their parent materials such as satisfactory biocompatibility and electronic properties, and were expected to be a promising host for enzyme loading and biosensing. The $CdSe_xTe_{1-x}$/Au nanotubes can provide a suitable microenvironment for protein and enhance direct electron transfer between the protein and underlying electrodes (Bao et al. 2008; Chen et al. 2009; Shan et al. 2009). In order to test the activity of $CdSe_xTe_{1-x}$/Au/Hb nanocomposites, their response to the reduction of H_2O_2 was examined. As shown in Fig. 6a, the i_{cat} values are linear with increasing concentration of H_2O_2 in the range from 2.0×10^{-6} mol L^{-1} to 2.0×10^{-4} mol L^{-1}. The linear regression equation was $y = 0.32847 + 0.0114x$, with a correlation coefficient of 0.99982 (Fig. 6b). The satisfactory reproducibility was observed using six Hb modified electrodes. The relative standard deviation was 2.8 % for the current determined at 50 μmol L^{-1} H_2O_2. Moreover, the biosensor could retain 97 % of its initial response after 20-days storage, suggesting a good stability. The AuNPs on the tubes offer suitable microenvironment for the immobilized protein; the semiconductor alloy nanotubes may act as electronic wires between the macroscopic electrode and the redox center of the protein to promote the direct electrochemistry (Cai et al. 2008). The excellent performance of the biosensor also demonstrates the feasibility of applying the $CdSe_xTe_{1-x}$/Au/Hb nanocomposites in biosensing.

Conclusions

In summary, we have developed a general sacrificial template method to fabricate $CdSe_xTe_{1-x}$ alloy nanotubes, and the ratio of Se and Te could be easily tuned by changing reaction parameters. AuNPs have been in situ assembled on the surface of nanotubes by a facile sonochemical route. The $CdSe_xTe_{1-x}$/Au nanotubes were further used for the loading of Hb to fabricate a biosensor, and it was found that the immobilized Hb exhibited fast direct electron transfer and good electrocatalytic performance to H_2O_2 with high sensitivity and wide linear range. The nanocomposite, with an interesting structure and unique features, might be a promising material for electronic, optical, and catalysis applications in the future.

Acknowledgments We greatly appreciate the support of National Natural Science Foundation of China (No. 21075061, 21103088, 21105021) and the National Basic Research Program of China (Grant 2011CB933502).

References

Bao SJ, Li CM, Zang JF, Cui XQ, Qiao Y, Guo J (2008) New nanostructured TiO2 for direct electrochemistry and glucose sensor applications. Adv Funct Mater 18:591–599

Cai WY, Xu Q, Zhao XN, Zhu JJ, Chen HY (2006) Porous gold-nanoparticle-CaCO3 hybrid material: preparation, characterization, and application for horseradish peroxidase assembly and direct electrochemistry. Chem Mater 18:279–284

Cai WY, Feng LD, Liu SH, Zhu JJ (2008) Hemoglobin-CdTe-CaCO3@ polyelectrolytes 3D architecture: fabrication, characterization, and application in biosensing. Adv Funct Mater 18:3127–3136

Chang S, Singamaneni S, Kharlampieva E, Young SL, Tsukruk VV (2009) Responsive hybrid nanotubes composed of block copolymer and gold nanoparticles. Macromolecules 42:5781–5785

Chen W, Cai WP, Liang CH, Zhang LD (2001) Synthesis of gold nanoparticles dispersed within pores of mesoporous silica induced by ultrasonic irradiation and its characterization. Mater Res Bull 36:335–342

Chen X, Zhang JJ, Xuan J, Zhu JJ (2009) Myoglobin/gold nanoparticles/carbon spheres 3-D architecture for the fabrication of a novel biosensor. Nano Res 2:210–219

Cui RJ, Huang HP, Yin ZZ, Gao D, Zhu JJ (2008a) Horseradish peroxidase-functionalized gold nanoparticle label for amplified immunoanalysis based on gold nanoparticles/carbon nanotubes hybrids modified biosensor. Biosens Bioelectron 23:1666–1673

Cui RJ, Liu C, Shen JM, Gao D, Zhu JJ, Chen HY (2008b) Gold nanoparticle-colloidal carbon nanosphere hybrid material: preparation, characterization, and application for an amplified electrochemical immunoassay. Adv Funct Mater 18:2197–2204

Ding J, Wang X, Zhuo LH, Tang B (2009) Hierarchical assembly of CdTe nanotubes and nanowires at water–oil interface. J Mater Chem 19:3027–3032

Farvid SS, Wang T, Radovanovic PV (2011) Colloidal gallium indium oxide nanocrystals: a multifunctional light-emitting phosphor broadly tunable by alloy composition. J Am Chem Soc 133:6711–6719

Huang Y, Sun F, Wang H, He Y, Li L, Huang Z, Wu Q, Yu JC (2009) Photochemical growth of cadmium-rich CdS nanotubes at the air-water interface and their use in photocatalysis. J Mater Chem 19:6901–6906

Jha N, Ramaprabhu S (2010) Development of Au nanoparticles dispersed carbon nanotube-based biosensor for the detection of paraoxon. Nanoscale 2:806–810

Jia F, Shan CS, Li FH, Niu L (2008) Carbon nanotube/gold nanoparticles/polyethylenimine-functionalized ionic liquid thin film composites for glucose biosensing. Biosens Bioelectron 24:945–950

Liang GX, Gu MM, Zhang JR, Zhu JJ (2009a) Preparation and bioapplication of high-quality, water-soluble, biocompatible, and near-infrared-emitting CdSeTe alloyed quantum dots. Nanotechnology 20:415103–415111

Liang HW, Liu S, Gong JY, Wang SB, Wang L, Yu SH (2009b) Ultrathin Te nanowires: an excellent platform for controlled synthesis of ultrathin platinum and palladium nanowires/nanotubes with very high aspect ratio. Adv Mater 21:1850–1854

Liu SH, Xing RM, Lu F, Rana RK, Zhu JJ (2009) One-pot template-free fabrication of hollow magnetite nanospheres and their application as potential drug carriers. J Phys Chem C 113:21042–21047

Liu SH, Lu F, Jia XD, Cheng FF, Jiang LP, Zhu JJ (2011) Microwave-assisted synthesis of a biocompatible polyacid-conjugated Fe_3O_4 superparamagnetic hybrid. CrystEngComm 13:2425–2429

Lo PK, Altvater F, Sleiman HF (2010) Templated synthesis of dna nanotubes with controlled, predetermined lengths. J Am Chem Soc 132:10212–10214

Mercuri F, Leoni S, Green JC, Wilson M (2010) Atomistic engineering in the control of the electronic properties of CdSe nanotubes. Phys Rev B 82:155429

Miao JJ, Ren T, Dong L, Zhu JJ, Chen HY (2005) Double-template synthesis of CdS nanotubes with strong electrogenerated chemiluminescence. Small 1:802–805

Miao JJ, Jiang LP, Liu C, Zhu JM, Zhu JJ (2007) General sacrificial template method for the synthesis of cadmium chalcogenide hollow structures. Inorg Chem 46:5673–5677

Mizukoshi Y, Tsuru Y, Tominaga A, Seino S, Masahashi N, Tanabe S, Yamamoto TA (2008) Sonochemical immobilization of noble metal nanoparticles on the surface of maghemite: mechanism and morphological control of the products. Ultrason Sonochem 15:875–880

Pradhan A, Jones RC, Caruntu D, O'Connor CJ, Tarr MA (2008) Gold–magnetite nanocomposite materials formed via sonochemical methods. Ultrason Sonochem 15:891–897

Qiu LH, Pol VG, Wei Y, Gedanken A (2004) Sonochemical decoration of multi-walled carbon nanotubes with nanocrystalline tin. New J Chem 28:1056–1059

Rao CNR, Govindaraj A, Deepak FL, Gunari NA, Nath M (2001) Surfactant-assisted synthesis of semiconductor nanotubes and nanowires. Appl Phys Lett 78:1853–1855

Ren R, Leng CC, Zhang SS (2010) A chronocoulometric DNA sensor based on screen-printed electrode doped with ionic liquid and polyaniline nanotubes. Biosens Bioelectron 25:2089–2094

Shan CS, Yang HF, Song JF, Han DX, Ivaska A, Niu L (2009) Direct electrochemistry of glucose oxidase and biosensing for glucose based on graphene. Anal Chem 81:2378–2382

Shen QM, Jiang LP, Miao JJ, Hou WH, Zhu JJ (2008) Sonoelectrochemical synthesis of CdSe nanotubes. Chem Commun 14:1683–1685

Shim HS, Shinde VR, Kim JW, Gujar TP, Joo OS, Kim HJ, Kim WB (2009) Diameter-tunable CdSe nanotubes from facile solution-based selenization of Cd(OH)2 nanowire bundles for photoelectrochemical cells. Chem Mater 21:1875–1883

Wang J, Han H (2010) Hydrothermal synthesis of high-quality type-II CdTe/CdSe quantum dots with near-infrared fluorescence. J Colloid Interface Sci 351:83–87

Wang L, Niu MG, Wu ZW (2009) In situ growth of CdSe/CdS quantum dots inside and outside of MWCNTs. Curr Appl Phys 9:1112–1116

Xia Y, Yang P, Sun Y, Wu Y, Mayers B, Gates B, Yun Y, Kim F, Yan H (2003) One-dimensional nanostructures: synthesis, characterization, and applications. Adv Mater 15:353–389

Xiao XL, Luan QF, Yao X, Zhou KB (2009) Single-crystal CeO_2 nanocubes used for the direct electron transfer and electrocatalysis of horseradish peroxidase. Biosens Bioelectron 24:2447–2451

Yang J, Zhang RY, Xu Y, He PG, Fang YZ (2008) Direct electrochemistry study of glucose oxidase on Pt nanoparticle-modified aligned carbon nanotubes electrode by the

assistance of chitosan-CdS and its biosensoring for glucose. Electrochem Commun 10:1889–1892

Yang Y, Yang RB, Fan HJ, Scholz R, Huang ZP, Berger A, Qin Y, Knez M, Gosele U (2010) Diffusion-facilitated fabrication of gold-decorated Zn2SiO4 nanotubes by a one-step solid-state reaction. Angew Chem Int Ed 49: 1442–1446

Zeng RS, Zhang TT, Liu JC, Hu S, Wan Q, Liu XM, Peng ZW, Zou BS (2009) Aqueous synthesis of type-II CdTe/CdSe core-shell quantum dots for fluorescent probe labeling tumor cells. Nanotechnology 20:095102–095109

Zhai T, Fang X, Bando Y, Liao Q, Xu X, Zeng H, Ma Y, Yao J, Golberg D (2009) Morphology-dependent stimulated emission and field emission of ordered CdS nanostructure arrays. ACS Nano 3:949–959

Zhang L, Zhang Q, Li JH (2007a) Layered titanate nanosheets intercalated with myoglobin for direct electrochemistry. Adv Funct Mater 12:1958–1965

Zhang L, Zhang Q, Lu XB, Li JH (2007b) Direct electrochemistry and electrocatalysis based on film of horseradish peroxidase intercalated into layered titanate nano-sheets. Biosens Bioelectron 23:102–106

Zhang HF, Meng ZC, Wang Q, Zheng JB (2011) A novel glucose biosensor based on direct electrochemistry of glucose oxidase incorporated in biomediated gold nanoparticles–carbon nanotubes composite film. Sens Actuators B 158:23–27

Zhao HY, Xu XX, Zhang JX, Zheng W, Zheng YF (2010) Carbon nanotube-hydroxyapatite-hemoglobin nanocomposites with high bioelectrocatalytic activity. Bioelectrochemistry 78:124–129

Zhou M, Zhu H, Wang X, Xu Y, Tao Y, Hark S, Xiao X, Li Q (2009) CdSe nanotube arrays on ITO via aligned ZnO nanorods templating. Chem Mater 22:64–69

Zhu HM, Yang BF, Xu J, Fu ZP, Wen MW, Guo T, Fu SQ, Zuo J, Zhang SY (2009) Construction of Z-scheme type CdS-Au-TiO2 hollow nanorod arrays with enhanced photocatalytic activity. Appl Catal B Environ 90:463–469